SEGMENTATION OF ANATOMICAL BRANCHING STRUCTURES BASED ON TEXTURE FEATURES AND GRAPH CUT

Tatyana Nuzhnaya[1], Erkang Cheng[2], Haibin Ling[2], Despina Kontos[3], Predrag R. Bakic[3], Vasileios Megalooikonomou[1]

[1]Data Engineering Laboratory (DEnLab), [2]Center for Information Science and Technology, Temple University, 1805 N. Broad St. Philadelphia, PA 19122, USA

[3]Department of Radiology, University of Pennsylvania, 3400 Spruce St., Philadelphia, PA 19104, USA

ABSTRACT

Segmentation of tree-like structure within medical imaging modalities, such as x-ray, MRI, ultrasound, etc., is an important step for analyzing branching patterns involved in many anatomic structures. However, images acquired using these different acquisition techniques frequently have features of poor contrast, blurring and noise, and therefore the segmentation result of traditional image segmentation methods may not be satisfactory. In this paper, we propose a framework for accurate segmentation of the ductal network in x-ray galactograms. Our approach is based on the graph cut algorithm and texture analysis to extract features of skewness, coarseness, contrast, energy and fractal dimension. The features are chosen to capture not only architectural variability of the enhanced ductal tree, but also spatial variations among pixels. The proposed approach was applied to a dataset of 20 galactographic images. We performed receiver operating characteristic (ROC) curve analysis to assess the accuracy. The area under the ROC curve observed was 0.76, indicating that our approach may potentially assist clinicians in the interpretation of breast images and facilitate the investigation of relationships among structure and texture of the branching patterns.

Index Terms— Branching Structure, Breast Imaging, Graph cut, Texture features.

1. INTRODUCTION

Studies have previously associated the morphological variability of the breast ductal network with subsequent development of breast cancer, suggesting that analysis of branching structures within the human breast can assist in diagnosing malignancy or estimating cancer risk [1,7,13]. Locating branching patterns encountered not only in ductal network analysis, but also in analysis of bronchial, vascular and neuronal networks is a very important first step towards understanding the relationships between morphology and function of tree-like structures in the human body.

However, fully automatic segmentation in the medical imaging domain can be challenging due to the complexity of anatomical structures and obstacles introduced by the imaging process [7,8]. Such obstacles include blurring, noise and the vessel occlusion and intersection caused by 3D to 2D projection. Furthermore, there is variability within the manually segmented ductal network skeletons and vessel structures provided by the different experts.

Motivated by these challenges, in this study we developed an interactive semi-automatic framework for accurate segmentation of the ductal network in x-ray galactograms. We extended the graph cut algorithm [4] using texture analysis to incoporate features of skewness, coarseness, contrast, energy and fractal dimension, strengthening the segmentation results of the original method, and further illustrating the importance of texture in branching structure segmentation.

2. BACKGROUND

Many effective methods have been developed to detect and analyze the branching anatomic structures. For example, machine learning techniques have played an important role in studying branching anatomy. In [10], Adaboost learning has been applied on features for classification of lung bronchovascular anatomy. In [2] the authors have used support vector machines (SVM) as a probabilistic inference framework for branching node detection, which is an important step towards complete branching pattern segmentation.

Unfortunately, standard learning algorithms, such as SVM and logistic regression, combined with simple local image features, such as intensity and gradient, treat image pixels as independent. Hence, due to the complexity frequently encountered in medical images, such algorithms may have limited accuracy for automatic segmentation. Early on, researchers realized that human input could be valuable in the segmentation process, and can aid in obtaining more reliable and accurate results. This has led to the development of interactive methods like snake [5],

deformable templates [6] and more recent interactive graph cuts [4]. For example, in [11], a new graph cut-based segmentation algorithm is used for precise identification of breast tumor regions.

Breast images are often highly textural and several studies suggest that computer-extracted texture features could provide objective and reproducible methods to identify parenchymal patterns [12]. For example, the segmentation of ultrasound images based on texture features, obtained according to gray level co-occurrence matrix and graph cuts, was proposed in [3]. In our study we propose to extend the set of texture features used in the graph cut framework by including the fractal dimension in order to capture more accurate spatial relations between pixels in the image.

3. METHODOLOGY

3.1. Problem formulation

We perform image segmentation in the framework of graph cuts introduced by Boykov and Jolly in [4]. In this section, we describe only the basic ideas of the graph cut algorithm due to space limitations. The reader should refer to [4] for more detailed explanation.

In short, for a given image I that has to be segmented into object and background, one can construct an undirected graph $G =< V, \varepsilon >$, where V is a set of vertices and ε a set of edges. Each graph is assigned two terminal nodes, source S and sink T, corresponding to the object and background respectively. Other nodes in the graph represent the pixels of the image p. The edges (links) characterize spatial relations between nodes in the graph. There are two types of links: n-links (neighborhood links denoted as $\{p,q\}$) and t-links (edges from terminals to the pixels, $\{p,S\}$ and $\{p,T\}$). All edges ε are assigned the nonnegative weights w_ε, which are used to construct a meaningful energy function. The calculation of the weights is based on pixel intensities and texture features of coarseness, skewness, contrast, energy and fractal dimension. After the computation of the energy function, the next step is to compute the graph cut corresponding to the optimal segmentation result. In order to obtain the minimum cut, one should solve the energy function minimization problem. Finally, the segmentation of the images is computed using (2).

The rest of this paper is organized as follows. Section 3.2 introduces image texture features used for computation of the weights needed for the energy function computation. Section 3.3 introduces more details of the graph cuts segmentation algorithm. Our experimental results on a set of x-ray galactograms are shown in Section 4. In Section 5 we give our conclusions.

3.2. Texture feature extraction

Texture features were extracted from a region of interest (ROI) containing part of the ductal network that was manually segmented for each of the x-ray galactograms. To characterize the parenchymal pattern, texture features of skewness, coarseness, contrast, energy, and fractal dimension (FD), were estimated from all the ROIs. These texture features were originally defined for 2D image analysis and have been previously used for breast cancer risk assessment in studies with digital mammograms [8, 12]. Skewness is the third statistical moment and is computed as

$$skewness = \frac{w_3}{w_2^{\frac{3}{2}}}, w_k = \sum_{i=0}^{g_{max}} \frac{n_i (i-\bar{\imath})^k}{N}, \sum_{i=0}^{g_{max}} n_i,\ \bar{\imath} = \sum_{i=0}^{g_{max}} \frac{in_i}{N},$$

where n_i represents the number of times that gray-level value i occurs in the image region, g_{max} is the maximum gray-level value, and N is the total number of image pixels.

Coarseness computation is based on the Neighborhood Gray Tone Difference Matrix(NGTDM) [12] of the gray-level values within the image region; this matrix is derived by estimating the difference between the gray-level value of each pixel and the average gray-level value of the pixels around a neighborhood window:

$$coarsness = \left(\sum_{i=0}^{g_{max}} p_i v(i),\right)^{-1},\ v(i) = \begin{Bmatrix} \sum |i - \bar{L_\iota}|, n_i \neq 0 \\ 0,\ n_i = 0\ , i \in \{n_i\} \end{Bmatrix},$$

where $v(i)$ is the NGTDM, p_i is the probability that gray level i occurs, $\{n_i\}$ is the set of pixels having gray-level values equal to i, and L_i is given by

$$L_i = \frac{1}{S-1} \sum_{k=-t}^{t} \sum_{l=-t}^{t} j(x+k, y+l),$$

where $j(x,y)$ is the pixel located at (x,y) with gray-level value i, $(k,l) \neq (0,0)$, and $S=(2t+1)^2$, with $t = 1$ specifying the neighborhood size around the pixel located at (x,y).

Contrast and energy, as proposed originally by Haralick et al [19], require the computation of second-order statistics derived from the gray-level co-occurrence matrix; the spatial dependence of gray levels is estimated by calculating the frequency of the spatial co-occurrence of gray levels in the image:

$$contrast = \sum_{i=0}^{g_{max}} \sum_{j=0}^{g_{max}} |i-j|^2 Q(i,j),$$
$$energy = \sum_{i=0}^{g_{max}} \sum_{j=0}^{g_{max}} Q(i,j)^2,$$

where Q is the normalized co-occurrence matrix.

The FD was estimated on the basis of the power spectrum of the Fourier transform of the image. The 2D discrete Fourier transform was performed using the fast-Fourier transform (FFT) algorithm as:

$$F(u,v) = \sum_{m=0}^{M-1} \sum_{n=0}^{N-1} I(m,n) e^{-j\left(\frac{2\pi}{M}\right)um} e^{-j\left(\frac{2\pi}{N}\right)vn},$$

where I is the region of size (M,N), and u and v are the spatial frequencies in the x and y directions, $u=\{1..M-1\}$, $v=\{1..N-1\}$. The power spectral density, P, was estimated from $F(u,v)$ as

$$P(u,v) = |F(u,v)|^2.$$

To compute the FD, P was averaged over radial slices spanning the FFT frequency domain.

Since the texture features of a single pixel cannot be computed, we calculated the texture features of a region known as the texture window. A 3 × 3 texture window or an 8-neigborhood was used in our study.

3.3. Graph cuts segmentation

We manually label sets of pixels as object and background. Let *Ob* and *Bk* denote the subsets of pixels labeled as "object" and "background" respectively. For the set P of all pixels p of image I, the subsets $Ob \subset P$ and $Bk \subset P$ are labeled so that $Ob \cap Bk = \emptyset$.

Let $A = (A_1, \ldots, A_p, \ldots, A_{|P|})$ be a binary vector whose components A_p specify assignments to pixels p in P. Each $A_p \subset Ob$ or $A_p \subset Bk$. Vector A defines a segmentation.

The constraints imposed on boundary and region properties of A are described by the energy function $E(A)$:

$$E(A) = \lambda R(A) + B(A), \quad (1)$$

where, λ denotes the relative importance of the region properties term $R(A)$ versus the boundary properties term $B(A)$. The details are explained in [4]. In our study, regions are represented by the 8-neighborhoods of the image pixels. The penalties are assigned according to discontinuities between pixels of similar intensities and texture.

The histogram distributions $H(I_p|Ob)$ and $H(I_p|Bk)$, where I_p are the intensities of the pixels are used to compute a set of regional penalties $R(.)$ as follows:

$$R_p(Ob) = -lnH(I_p|Ob), \; R_p(Bk) = -lnH(I_p|Bk).$$

The boundary penalties between pixels p and q are computed based on the texture features, described in Section 3.2, as well as intensity of the pixels as follows:

$$B_{\{p,q\}} \propto \exp\left(-\frac{\sum_{all\ features} ||F_p - F_q||^2}{2\delta_F^2}\right) \cdot \frac{1}{dist(p,q)},$$

$$F = (skewness, coarseness, contrast, energy, FD, intensity)'$$

This function penalizes a lot for discontinuities between pixels with similar features when $|F_p - F_q| < \delta_F$. If the difference between the features is large, then the penalty is small. δ_F is the standard deviation of the feature F on the whole image I. The weights are computed according to Table 1, where $K = 1 + \max_{p \in P} \sum_{q:\{p,q\} \in N} B_{\{p,q\}}$.

edge	*weight*	*case*
{p,q}	$B_{\{p,q\}}$	$\{p,q\} \in neigborhood$
{p,S}	0	$p \in Bk$
	K	$p \in Ob$
	$\lambda \cdot R_p(Bk)$	$p \in P$
{p,T}	0	$p \in Ob$
	K	$p \in Bk$
	$\lambda \cdot R_p(Ob)$	$p \in P$

Table 1. Computation of the edge weights.

After the weights are computed, the energy function is calculated by (1). The graph cut is defined as a subset of edges $C \subset \varepsilon$. The cost of the cut is $|C| = \sum_{e \in C} w_e$, where e are the edges in the cut and w_e are their weights. [4] provides a proof that the minimum graph cut can be found by minimizing the energy function. As a final step, a unique segmentation corresponding to the cut is computed as

$$A_p(C) = \begin{cases} Ob, if\ \{p,T\} \in C \\ Bk, if\ \{p,S\} \in C \end{cases}. \quad (2)$$

The details of the procedure are described in [4].

4. EXPERIMENTAL RESULTS

To test the proposed approach, we used a dataset containing 20 X-ray galactograms. The ROI containing the ductal network was manually segmented from the central breast region behind the nipple (i.e., the retroareolar region) in each of the 20 breast images. All the branching structures had been manually segmented and skeletons annotated by the experts. An example of an X-ray galactogram and an annotated skeleton of the ductal network and background seeds is shown in Figure 1.

In the original image (Figure 1(a)), the boundaries of the ducts are unclear; therefore, it is difficult to segment the tree-like structure using edge detection based on grey-level intensity. Figure 2(a) shows the segmentation of the ducts performed by the expert. It is used as a ground truth to compare different segmentation results. Note that the results of manual segmentation provided by the different experts may vary. A segmentation of the network by the original graph cut with gray-level intensity is shown in Figure 2(b). Finally, in Figure 2(c) we present the segmentation result obtained by our method.

From the segmentation results, it is easy to see that the graph cut algorithm can obtain better results when combined with various texture features. The method becomes more effective when including texture features that provide more spatial information than gray-level intensity alone.

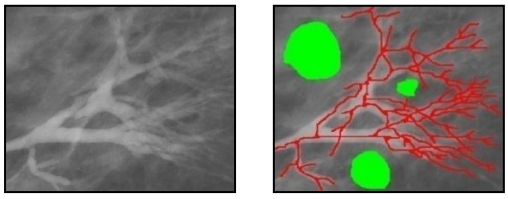

(a) (b)

Fig. 1: (a) An original X-ray galactogram, (b) expert annotated ductal network and 3 background seeds.

Figure 3 presents an average ROC curve after the first run of the graph cuts algorithm, with three initial background seeds. The true positive rate measures the proportion of pixels that were identified by the algorithm as a part of ductal network and which are manually segmented by the expert as such. The false positive rate reflects the

percentage of the pixels that are classified as a part of background and which are manually identified as a surrounding tissue by the medical expert. The average area under the ROC curve over all experiments was 0.76; demonstrating promising preliminary results that can potentially speed up and improve the accuracy of the tedious manual segmentation task.

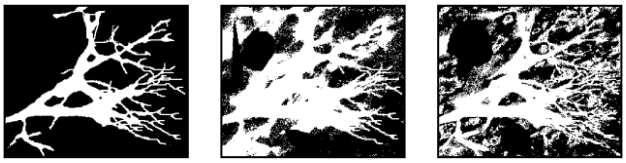

(a) (b) (c)

Fig. 2: (a) manual expert segmentation of the vessels, (b) segmentation based on the original graph cut method, (c) segmentation based on the proposed graph cut algorithm with skewness, coarseness, contrast, energy and fractal dimension features.

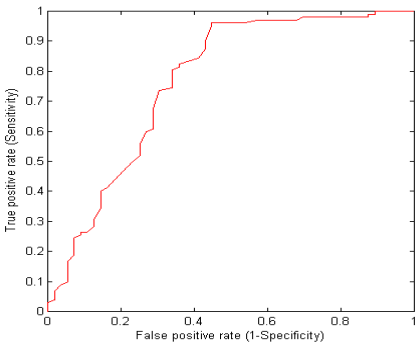

Fig. 3: The average ROC curve after the first run of the graph cuts algorithm using three background seeds.

5. CONCLUSION

In this paper, we presented a framework for the semi-automatic segmentation of the breast ductal network from x-ray galactograms. We focused on characterizing the actual topology of the ductal network using the texture features of skewness, coarseness, contrast, energy and fractal dimension. The well-known graph cut algorithm was used as a segmentation tool. Our experimental results show that the performance of the algorithm is significantly improved with the use of texture features. ROC curve analysis was performed to assess the accuracy of the segmentation algorithm in discriminating between the ductal network and its' surrounding tissue. The average ROC performance obtained on a dataset containing 20 breast images was 0.76, demonstrating promising preliminary results and indicate that with further improvements our method can potentially aid the tedious manual segmentation task. In our future work we plan to study the effect of each individual feature on the improvement of segmentation and perform more objective comparisons using Dice scores.

6. ACKNOWLEDGMENTS

This work was supported by NSF Research Grants IIS-0237921 and IIS-0916624. The funding agency specifically disclaims responsibility for any analyses, interpretations and conclusions.

7. REFERENCES

[1] G. Cardenosa, C. Doudna, G.W. Eklund, "Ductography of the breast: technique and findings," Am. J. Roentgenol., May 1994, Vol. 162, pp. 1081 - 1087.

[2] T. Nuzhnaya, M. Barnathan, H. Ling, etc. "Probabilistic Branching Node Detection Using AdaBoost and Hybrid Local Features", ISBI, 2010.

[3] K. Sikka, T.M. Deserno. "Segmentation of Ultrasound Image Based on Texture Feature and Graph Cut", CSSE, Vol. 1, pp.795-798, 2008.

[4] Y. Boykov, M. P. Jolly. "Interactive Graph cuts for optimal Boundary and Region Segmentation of Object in N-D Images", ICCV, Vol. I, pp.105-112, 2001.

[5] M. Kass, A. Witkin, and D. Terzolpoulos. "Snakes: Active contour models," IJCV, Vol.2, pp.321-331, 1998.

[6] E.N. Mortensen and W.A. Barrett. "Interactive segmentation with intelligent scissors," Graphical Models and Image Processing, Vol.60, pp.349-384, 1998.

[7] V. Megalooikonomou, M. Barnathan, D. Kontos, etc, "A Representation and Classification Scheme for Tree-like Structures in Medical Images: Analyzing the Branching Pattern of Ductal Trees in X-ray Galactograms," IEEE TMI, Vol. 28- 4, pp. 487-493, 2009.

[8] D. Kontos, P.R. Bakic, A.D.A. Maidment, "Analysis of Parenchymal Texture Properties in Breast Tomosynthesis Images," SPIE, 2007.

[9] R. M. Haralick, K. Shanmugam, and I. Dinstein, "Textural Features of Image Classification," IEEE Transactions on Systems, Man and Cybernetics, Vol. 3- 6, pp. 610-621, 1973.

[10] R. A. Ochs, J. G. Goldin, F. Abtin, etc, "Automated classification of lung bronchovascular anatomy in CT using AdaBoost," Medical Image Analysis, Vol. 11-3, pp. 315-324,2007.

[11] Y. Zheng, S. Baloch, S. Englander, etc, "Segmentation and Classification of Breast Tumor Using Dynamic Contrast-Enhanced MR Images," MICCAI, Vol. 4792, pp. 393–401, 2007.

[12] H. Li, M.L. Giger, O.I. Olopade, etc, "Computerized texture analysis of mammographic parenchymal patterns of digitized mammograms," Acad Radiol, Vol. 12, pp. 863–873, 2005.

[13] P.R. Bakic, M. Albert, A.D. Maidment, "Classification of galactograms with ramification matrices: preliminary results", Academic Radiology, Vol. 10 (2), pp. 198-204, 2003.